

Synthesis of Terminal and Bridging Acetonyl Complexes of Palladium(II). Crystal Structures of $[\{(AsPh_3)(C_6F_5)Pd\}_2\{\mu-CH_2C(O)CH_3\}_2]$, $[(AsPh_3)(C_6F_5)Pd\{CH_2C(O)CH_3\}(t-BuNC)]$, and $[(o-C_6H_4CH_2NMe_2)Pd\{O,O'-CH(CO_2Et)_2\}]$

José Ruiz, Venancio Rodríguez, Natalia Cutillas, Mercedes Pardo, José Pérez, and Gregorio López*

Departamento de Química Inorgánica, Universidad de Murcia, 30071- Murcia, Spain

Penny Chaloner and Peter B. Hitchcock

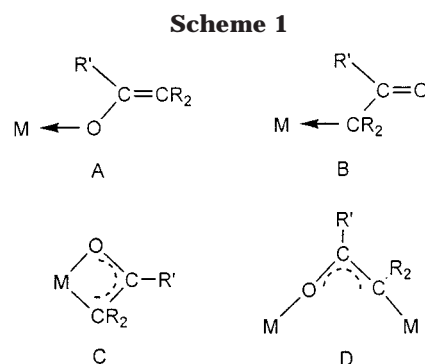
School of Chemistry, Physics and Environmental Science, University of Sussex, Brighton BN1 9QJ, U.K.

Received October 10, 2000

The reaction of the palladium-hydroxo complex $[(o-C_6H_4CH_2NMe_2)Pd]_2(\mu-OH)_2$ with acetone leads to the formation of the bridging O,C-acetonyl complexes $[(o-C_6H_4CH_2NMe_2)Pd]_2(\mu-OH)\{\mu-CH_2C(O)CH_3\}$ (**1**) and $[(o-C_6H_4CH_2NMe_2)Pd]_2\{\mu-CH_2C(O)CH_3\}_2$ (**2**). The reaction (1:2 molar ratio) of $[\{(AsPh_3)(C_6F_5)Pd\}_2(\mu-Cl)]_2$ with 20% aqueous $[NBu_4]OH$ in acetone yields $[\{(AsPh_3)(C_6F_5)Pd\}_2\{\mu-CH_2C(O)CH_3\}_2]$ (**3**). The reaction (1:1 ratio) between **2** or **3** and *t*-BuNC gives the monomeric complexes $[(o-C_6H_4CH_2NMe_2)Pd\{CH_2C(O)Me\}(t-BuNC)]$ (**4**) and $[(AsPh_3)(C_6F_5)Pd\{CH_2C(O)CH_3\}(t-BuNC)]$ (**5**). Heating an acetone solution of $[NBu_4][\{(C_6F_5)_2Pd\}_2(\mu-OH)_2]$ gave the 2,4-dimethyl-1-oxapenta-1,3-dienyl palladium complex $[NBu_4][\{(C_6F_5)_2Pd\}_2(\eta^5-2,4-Me_2-C_4H_3O)]$ (**6**). The reaction of $[(o-C_6H_4CH_2NMe_2)Pd]_2(\mu-OH)_2$ with $CH_2(CO_2R)_2$ (*R* = Et, Me) leads to $[(o-C_6H_4CH_2NMe_2)Pd\{O,O'-CH(CO_2R)_2\}]$ (**7**, *R* = Me; **8**, *R* = Et). The crystal structures of **3**, **5**, and **8** have been established by X-ray diffraction studies. The structure of **3** shows the C,O-enolate anion bridging two palladium atoms with a head-to-tail arrangement. In the monomeric complex **5** the C-bound acetonyl is *trans* to triphenylarsine. In **8** the diethyl malonate ligand and the palladium atom form a six-membered chelate ring.

Introduction

Transition metal enolates have been proposed as intermediates in numerous organic transformations.^{1–8} The term enolate is used as a generic name for the $CR_2C(=O)R'$ unit that can coordinate to a metal atom either through the oxygen atom (common for the oxophilic early transition metals; A in Scheme 1) or through the carbon atom (common for the carbophilic late transition metals; B in Scheme 1). The chemistry associated with these two metal enolates are very different. The synthesis of C-bound metal enolates (B) is normally achieved by an oxidative addition reaction



* Corresponding author. E-mail: gll@um.es.

(1) Seebach, D. *Angew. Chem., Int. Ed. Engl.* **1988**, *27*, 1624.

(2) Tsuji, J. *J. Org. Chem.* **1987**, *52*, 2988.

(3) Godleski, S. A. In *Comprehensive Organic Synthesis*; Trost, B. M., Ed.; Pergamon: New York, 1991; Vol. 3, Chapter 3.3, p 611.

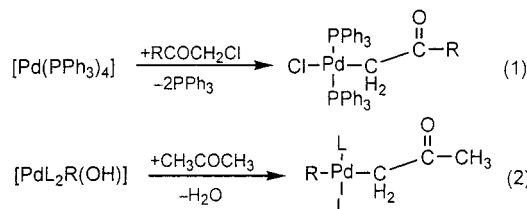
(4) Trost, B. M.; Verhoeve, T. R. In *Comprehensive Organometallic Chemistry*; Wilkinson, G., Stone, F. G. A., Abel, E. W., Eds.; Pergamon Press: Oxford, 1982; Vol. 8, p 838.

(5) Murahashi, S. I.; Mitsue, Y.; Tsumiyama, T. *Bull. Chem. Soc. Jpn.* **1987**, *60*, 3285.

(6) Ito, Y.; Hirao, T.; Saegusa, T. *J. Org. Chem.* **1978**, *43*, 1011.

(7) Mitsudo, T.; Kadokura, M.; Wantanabe, Y. *J. Org. Chem.* **1987**, *52*, 3186.

(8) Minami, I.; Nisar, M.; Yuhara, M.; Shimizu, I.; Tsuji, J. *Synthesis* **1987**, *11*, 992.



to a low-valent metal, and they undergo typical reactions of metal alkyls, but the presence of a nucleophilic site (oxygen) may also make them prone to electrophilic attack. As expected for a carbophilic metal, enolates

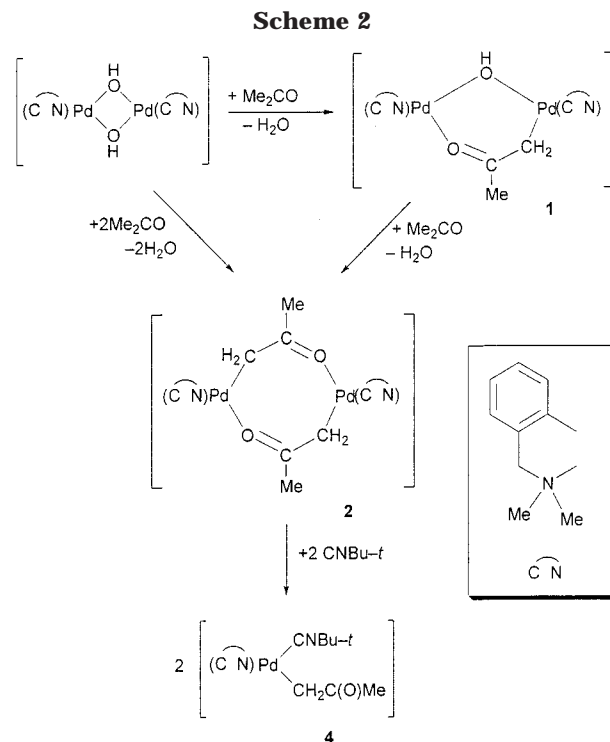
prefer to coordinate to palladium in the binding mode B,^{9–15} but the chelating η^3 -oxoallyl (C, Scheme 1)^{16–19} and bridging C–O (D, Scheme 1)^{11,20} modes are also found. The O-bound type A (Scheme 1) has also been proposed.²¹ Although palladium has been widely used for assisting the reactivity of enolate species, the number of isolated and well-characterized complexes is, however, rather limited.

The most convenient way of preparation of palladium enolates is the oxidative addition of haloketones to a Pd(0) complex (eq 1, Scheme 1).^{11,15,20,22,23} However, Pd–acetyl (methyl enolate) complexes have also been prepared by reacting acetone with hydroxo complexes (eq 2, Scheme 1).^{24–27}

Following our systematic study of the reactivity of di- μ -hydroxo complexes of the group 10 metals toward weak, protic electrophiles, we have now found that these dimeric compounds are very convenient starting materials for the preparation of Pd–acetyl complexes based on the acid–base reaction between the basic $>\text{Pd}(\mu\text{-OH})_2\text{M} <$ complex and Me_2CO . Bridging C,O-bound and terminal C-bound acetyl complexes can be prepared and, under appropriate conditions, acetone undergoes aldol condensation to give 2,4-dimethyl-1-oxapenta-1,3-dienyl at a palladium site. We report here the first crystal structures of a mononuclear and a binuclear palladium–acetyl complex.

Results and Discussion

μ -Acetyl Palladium Complexes $[(\text{o-C}_6\text{H}_4\text{CH}_2\text{NMe}_2)\text{Pd}]_2(\mu\text{-OH})\{\mu\text{-}\kappa^2\text{-C,O-CH}_2\text{C(O)CH}_3\}$ and $[(\text{o-C}_6\text{H}_4\text{CH}_2\text{NMe}_2)\text{Pd}]_2(\mu\text{-}\kappa^2\text{-C,O-CH}_2\text{C(O)CH}_3)_2$. The reaction of the hydroxo palladium complex²⁸ $[(\text{o-C}_6\text{H}_4\text{CH}_2\text{NMe}_2)\text{Pd}(\mu\text{-OH})]_2$ with acetone under reflux leads (Scheme 2) to the formation of the bridging O,C-bound acetyl complexes $[(\text{o-C}_6\text{H}_4\text{CH}_2\text{NMe}_2)\text{Pd}]_2(\mu\text{-OH})\{\mu\text{-}\kappa^2\text{-C,O-CH}_2\text{C(O)CH}_3\}$ (**1**) and $[(\text{o-C}_6\text{H}_4\text{CH}_2\text{-}$



$\text{NMe}_2)\text{Pd}]_2\{\mu\text{-}\kappa^2\text{-C,O-CH}_2\text{C(O)CH}_3\}$ (**2**). These reactions imply proton abstraction from acetone by the hydroxo complex with the concomitant release of water. The formation of **1** or **2** depends on the reaction conditions used (30 min reflux or 4 h reflux, respectively), and both complexes may be obtained as pure samples. On protonation of the hydroxo complex, it is likely that an intermediate aqua complex is formed, but we have not been able to detect this species. The presence of the hydroxo ligand in complex **1** is manifested by the observation of the characteristic IR absorption at 3560 cm^{-1} (OH str) and a high-field proton resonance at $\delta -2.01$.^{28–30} The $\nu(\text{CO})$ absorptions are observed in the vicinity of 1560 cm^{-1} . The analysis of the ^1H NMR spectrum gave more structural information on **1**. Thus, the singlet signals observed in the ^1H NMR spectrum at $\delta 3.22$ and 2.24 are assignable to the methylene and methyl protons of the acetyl ligand, respectively, and in addition to the low-field resonances of the C_6H_4 groups, two singlet resonances for the N-Me groups (at $\delta 2.74$ and 2.67) and two singlet resonances for the CH_2 protons (at $\delta 3.81$ and 3.22) of bonded $\text{C}_6\text{H}_4\text{CH}_2\text{NMe}_2$ are observed, which indicate the presence of two inequivalent chelating C–N ligands. The $^{13}\text{C}\{^1\text{H}\}$ NMR spectrum shows signals at $\delta 41.6$ and 28.7 which are assignable to the methylene and methyl carbons of the acetyl ligand, but the CO resonance could not be observed. All these NMR data indicate that only one of the four possible geometrical isomers (Scheme 3) is present in solution. Moreover, the strong NOE observed between the CH_2CO protons and the aromatic H resonances of the bidentate $\text{C}_6\text{H}_4\text{CH}_2\text{NMe}_2$ ligand indicates the proximity of the interacting nuclei. This would not be possible for the isomers a and b in Scheme 3. The selective irradiation at $\delta -2.01$ produced a clear NOE

(9) Vicente, J.; Abad, J. A.; Chicote, M. T.; Abrisqueta, M. D.; Lorca, J. A.; Ramírez de Arellano, M. C. *Organometallics* **1998**, *17*, 1564.

(10) Burkhardt, E. R.; Bergman, R. G.; Heathcock, C. H. *Organometallics* **1990**, *9*, 30.

(11) Veya, P.; Floriani, C.; Chiesi-Villa, A.; Rizzoli, C. *Organometallics* **1993**, *12*, 4899.

(12) Suzuki, K.; Yamamoto, H. *Inorg. Chim. Acta* **1993**, *208*, 225.

(13) Byers, P. K.; Cauty, A. J.; Skelton, B. W.; Traill, P. R.; Watson, A. A.; White, A. H. *Organometallics* **1992**, *11*, 3085.

(14) Wanat, R. A.; Collum, D. B. *Organometallics* **1986**, *5*, 120.

(15) Bertani, R.; Castellani, C. B.; Crociani, B. *J. Organomet. Chem.* **1984**, *269*, C-15.

(16) Ito, Y.; Aoyama, H.; Hirao, T.; Mochizuki, A.; Saegusa, T. *J. Am. Chem. Soc.* **1979**, *101*, 494.

(17) Sodeoka, M.; Ohrai, K.; Shibasaki, M. *J. Org. Chem.* **1995**, *60*, 2648.

(18) Lemke, F. R.; Kubiak, C. P. *J. Organomet. Chem.* **1989**, *373*, 391.

(19) Yoshimura, N.; Murahashi, S.-I.; Moritani, I. *J. Organomet. Chem.* **1973**, *52*, C-58.

(20) Albéniz, A. C.; Catalina, N. M.; Espinet, P.; Redón, R. *Organometallics* **1999**, *18*, 5571.

(21) Fujii, A.; Hagiwara, E.; Sodeoka, M. *J. Am. Chem. Soc.* **1999**, *121*, 5450.

(22) Wanat, R. A.; Collum, D. B. *Organometallics* **1986**, *5*, 120.

(23) Yanase, N.; Nakamura, Y.; Kawaguchi, S. *Inorg. Chem.* **1980**, *19*, 1575.

(24) Yoshida, T.; Okano, T.; Otsuka, S. *J. Chem. Soc., Dalton Trans.* **1976**, 1945.

(25) Bennett, M. A.; Yoshida, T. *J. Am. Chem. Soc.* **1978**, *100*, 1750.

(26) Appleton, T. G.; Bennett, M. A. *Inorg. Chem.* **1978**, *17*, 738.

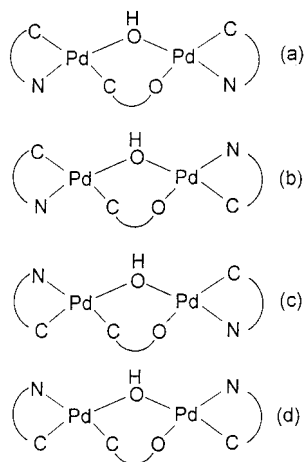
(27) Arnold, D. P.; Bennett, M. A. *J. Organomet. Chem.* **1980**, *199*, 119.

(28) Ruiz, J.; Cutillas, N.; Rodríguez, V.; Sampedro, J.; López, G.; Chaloner, P. A.; Hitchcock, P. *J. Chem. Soc., Dalton Trans.* **1999**, 2939.

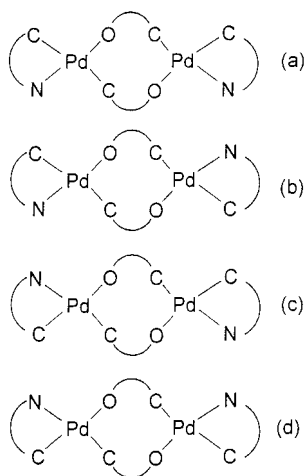
(29) López, G.; Ruiz, J.; García, G.; Vicente, C.; Casabó, J.; Molins, E.; Miravittles, C. *Inorg. Chem.* **1991**, *30*, 2605.

(30) Ruiz, J.; Cutillas, N.; Sampedro, J.; López, G.; Hermoso, J. A.; Martínez-Ripoll, M. *J. Organomet. Chem.* **1996**, *526*, 67.

Scheme 3



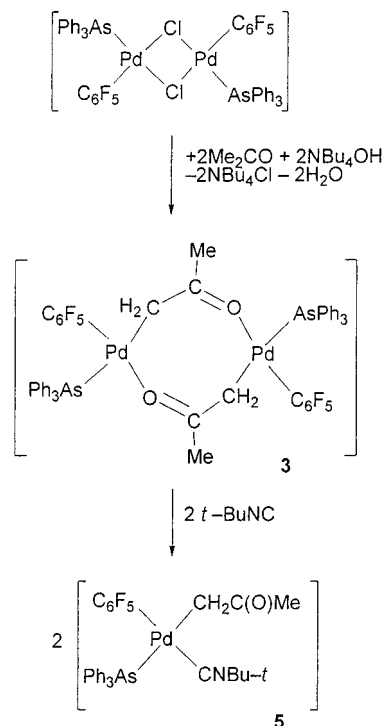
Scheme 4



enhancement of the aromatic signal at δ 6.9, which excludes isomer d. Therefore analysis of the NMR spectra including proton NOE difference spectra suggests that an *anti*-arrangement (c) is the most probable structure for this binuclear complex **1**. We found a similar *anti*-arrangement in the previously reported $[\text{Pd}_2(\text{PPh}_3)_2\text{Ph}_2(\mu\text{-OH})(\mu\text{-NHC}_6\text{H}_4\text{OMe-}p)]$.³¹

The IR spectrum of complex **2** shows a $\nu(\text{CO})$ absorption at 1566 cm^{-1} . The ^1H NMR spectrum is temperature dependent, showing broad resonances at room temperature. At $-20\text{ }^\circ\text{C}$ sharp resonances are observed, indicating that only one of the four possible geometrical isomers (a–d, Scheme 4) with a head-to-tail arrangement is present in solution at low temperature. The detailed NMR analysis including proton NOE difference spectra suggests that an *anti*-arrangement (c) is the most probable structure for this binuclear complex at low temperature. Two singlet resonances for the N-Me groups and an AB quartet ($J_{\text{AB}} = 13.8\text{ Hz}$) for the CH_2 protons of bonded $\text{C}_6\text{H}_4\text{CH}_2\text{NMe}_2$ are observed. This NMR pattern, which has been found in other related complexes such as $[(\text{O-C}_6\text{H}_4\text{CH}_2\text{NMe}_2)\text{Pd}]_2(\mu\text{-RC(O)-NH})_2$,²⁸ can be rationalized by assuming a frozen conformation of the Pd–N–C–C–C chelate ring or much slower interconversion of the conformations than the NMR time scale. The structure of **2** may be related

Scheme 5



to that of similar dinuclear acetylonyl complex **3** described below, which has a chair-type conformation of the eight-membered ring composed of Pd centers and bridging acetylonyl ligands. For the acetylonyl ligands a resonance at δ 2.24 for the methyl protons, which allows the discard of the *syn*-arrangements a and d shown in Scheme 4, and two resonances at δ 3.53 and 2.73 for the methylene protons are observed. The assignment of the CH_2CO resonances is confirmed by selective irradiation at δ 2.73, which produces a NOE enhancement of the signal at δ 3.53. Moreover, for complex **2** there is a strong NOE interaction from aromatic protons of the bidentate $\text{C}_6\text{H}_4\text{CH}_2\text{NMe}_2$ ligand to the CH_2CO resonances, indicating that the *O-trans*-to- NMe_2 geometry such as in d (Scheme 4) should be excluded. We suggest the *anti*-arrangement (c) for this binuclear complex where a CH_2 -*trans*-to- NMe_2 ligand geometry is present.

μ -Acetylonyl Palladium Complex $[(\text{AsPh}_3)(\text{C}_6\text{F}_5)\text{-Pd}]_2\{\mu\text{-}\kappa^2\text{-C, O-CH}_2\text{C(O)CH}_3\}_2$. The reaction of $[(\text{AsPh}_3)(\text{C}_6\text{F}_5)\text{Pd}]_2(\mu\text{-Cl})_2$ with 20% aqueous $[\text{NBu}_4]\text{-OH}$ (1:2 ratio) at room temperature, in acetone, yields $[(\text{AsPh}_3)(\text{C}_6\text{F}_5)\text{Pd}]_2\{\mu\text{-CH}_2\text{C(O)CH}_3\}_2$ (**3**) (Scheme 5). Although the formation of the acetylonyl derivative **3** could be thought to occur through the intermediacy of the hydroxo complex $[(\text{AsPh}_3)(\text{C}_6\text{F}_5)\text{Pd}]_2(\mu\text{-OH})_2$, we have proved that this is not the case. In fact $[(\text{AsPh}_3)(\text{C}_6\text{F}_5)\text{Pd}]_2(\mu\text{-OH})_2$ ³² was recovered unchanged after heating it under reflux in acetone for 2 h. We assume that in this case the acetylonyl ligands—generated in situ on deprotonation of the ketone by free OH^- —replace both chloro ligands from the starting complex with formation of **3** along with $[\text{NBu}_4]\text{Cl}$.

The IR spectrum of complex **3** shows the characteristic absorptions of the C_6F_5 group³³ at 1630, 1490, 1450, 1050, 950 and a single band at ca. 800 cm^{-1} , which is derived from the so-called X-sensitive mode³⁴ in C_6F_5 -halogen molecules and behaves like a $\nu(\text{M-C})$ band. The

(31) Ruiz, J.; Rodríguez, V.; López, G.; Chaloner, P. A.; Hitchcock, P. B. *J. Chem. Soc., Dalton Trans.* **1997**, 4271.

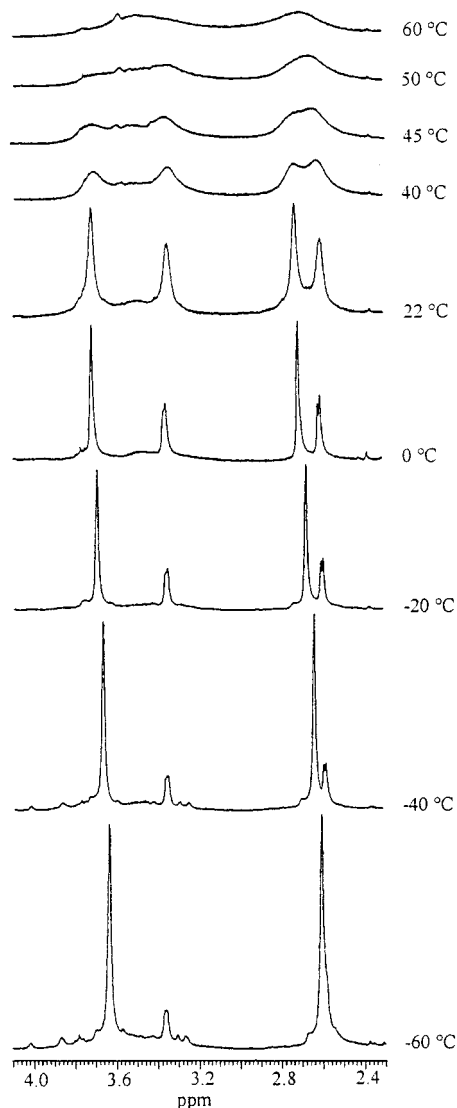


Figure 1. Variable-temperature ^1H NMR spectra of complex **3** in the CH_2 region.

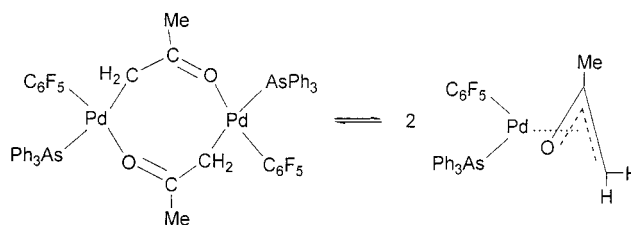
carbonyl stretching frequency for this palladium complex is found at 1554 cm^{-1} . The ^1H NMR spectrum of **3** in CDCl_3 is temperature dependent, showing broad resonances at room temperature. In fact, the variable-temperature ^1H NMR spectra (Figure 1) of a sample obtained by redissolution in CDCl_3 of white crystals of complex **3** (grown from toluene–hexane) indicate a rapid temperature-dependent equilibrium between two species. A process whereby the dimeric complex $[(\text{AsPh}_3)(\text{C}_6\text{F}_5)\text{Pd}]_2\{\mu\text{-CH}_2\text{C}(\text{O})\text{CH}_3\}_2$, in chloroform solution,

(32) The preparation of this complex is similar to that previously used for the triphenylphosphine analogue: Ruiz, J.; Vicente, C.; Martí, J. M.; Cutillas, N.; García, G.; López, G. *J. Organomet. Chem.* **1993**, *460*, 241. To a suspension of $[\text{Pd}_2(\text{C}_6\text{F}_5)_2(\text{AsPh}_3)_2(\mu\text{-Cl})_2]$ (250 mg; 0.203 mmol) in THF (15 mL) was added 20% aqueous $[\text{NBu}_4]\text{OH}$ (0.532 mL, 0.406 mmol), and the resulting solution was stirred at room temperature for 30 min and then the solvent was partially evaporated under reduced pressure. On addition of ethanol and a few drops of water, a pale yellow solid precipitated, which was filtered off and air-dried. Yield: 89%. Anal. Found: C, 48.5; H, 2.9. Calcd for $\text{C}_{32}\text{H}_{32}\text{F}_{10}\text{O}_2\text{As}_2\text{Pd}_2$: C, 48.3; H, 2.7. IR (Nujol, cm^{-1}): $\nu(\text{OH})$, 3602; $\text{Pd}-\text{C}_6\text{F}_5$ str, 794. ^1H NMR: δ 7.60–7.32 (15 H, AsPh₃), δ 1.49 (s, 2 H, OH). ^{19}F NMR: δ -117.3 (d, F_o , $J_{\text{om}} = 22.3\text{ Hz}$), -160.6 (t, F_p , $J_{\text{pm}} = 19.7\text{ Hz}$), -163.8 (m, F_m).

(33) Long, D. A.; Steel, D. *Spectrochim. Acta* **1963**, *19*, 1955.

(34) Maslowski, E. *Vibrational Spectra of Organometallic Compounds*; Wiley: New York, 1977; p 437.

Scheme 6



undergoes dissociation to give two monomers $[(\text{AsPh}_3)(\text{C}_6\text{F}_5)\text{Pd}\{\eta^3\text{-CH}_2\text{C}(\text{O})\text{CH}_3\}]$ can be proposed,³⁵ as shown in Scheme 6. The ^1H NMR spectrum (Figure 1) consists of four signals for the CH_2 group; the singlets at δ 3.70 and 2.70 are assigned to the dimer with a head-to-tail arrangement of the $\mu\text{-CH}_2\text{C}(\text{O})\text{CH}_3$ ligands and the two doublets at δ 3.35 and 2.62 to the $\eta^3\text{-CH}_2\text{C}(\text{O})\text{CH}_3$ ligand of the monomer. The observed NMR pattern is a consequence of the absence of a molecular symmetry plane. The dimer:monomer ratio increases as the temperature decreases. The weak signals observed at lower temperatures (-40 and -60 °C, Figure 1) are probably due to the presence of other dimeric isomers similar to those shown in Scheme 3. The ^{19}F NMR spectrum of **3** at 25 °C (Figure 2) is consistent with the above ^1H NMR data. The two triplets of the *para*-fluorine atoms indicate the presence of two different C_6F_5 groups, and the *ortho*- and *meta*-fluorine resonances are duplicated because there is no molecular mirror plane. Variable-temperature ^{19}F NMR studies for a solution of 20 mg of **3** in 0.7 mL of CDCl_3 show a dimer:monomer ratio of 1.6:1 at 233 K. As the temperature is raised, the relative proportion of monomer increases. The equilibrium constant (K_{eq}) over the range 233–283 K fits a linear plot of $\ln K_{\text{eq}}$ versus $1/T$, which gives $\Delta H = 19.8\text{ kJ mol}^{-1}$ and $\Delta S = 40\text{ J K}^{-1}\text{ mol}^{-1}$. The positive value observed for ΔS agrees with the presence of a dissociative process in solution.³⁶

The crystal structure of **3** has been established by X-ray diffraction. A view of the molecule is given in Figure 3. There are two independent molecules in the unit cell. Each of these lies on an inversion center, so that in the solid state at least the aryl rings are equivalent in the dimers. Selected bond lengths and angles are given in Table 1. The complex is a dinuclear unit where two enolato anions bridge two $\{\text{Pd}(\text{C}_6\text{F}_5)(\text{AsPh}_3)\}$ fragments with a head-to-tail arrangement and an *anti*-structure. The oxygen atom is *trans* to the pentafluorophenyl ligand in each case. Coordination geometry at palladium is approximately square planar. The eight-membered ring formed by the bridging enolate ligands adopts an approximately chairlike conformation. Although a number of bridging enolato complexes of palladium^{37,38} and other metals^{39,40} have been structurally characterized, in most of these the enolato ligand is part of a larger, often geometrically constrained or chelating group. The only comparable species for which a structure is available is $[\{\text{Pd}(\text{PPh}_3)_2\}_2(\mu\text{-}\{\text{CH}_2\text{-C}(\text{Ph})=\text{O}-\text{O}, \text{C}\})_2][\text{CF}_3\text{SO}_3]_2$.¹¹ This also shows distorted square planar geometry at palladium, but the eight-membered ring adopts a distorted boat conformation.

(35) Slough, A.; Hayashi, R.; Ashbaugh, J. R.; Shamblyn, S. L.; Aukamp, A. M. *Organometallics* **1994**, *13*, 890.

(36) Gupta, M.; Cramer, R. E.; Kachum, O.; Pettersen, C.; Mishina, S.; Belli, J.; Jensen, C. M. *Inorg. Chem.* **1995**, *34*, 60.

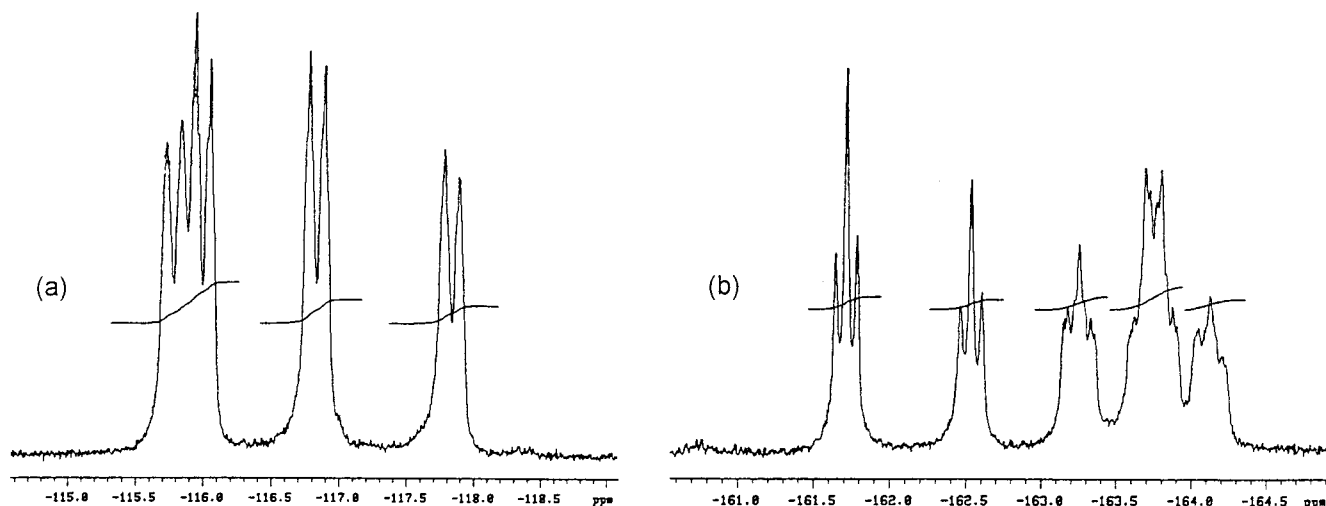


Figure 2. ^{19}F NMR spectrum at 25 °C of complex **3**: (a) *ortho*-fluorine region; (b) *para*- and *meta*-fluorine region.

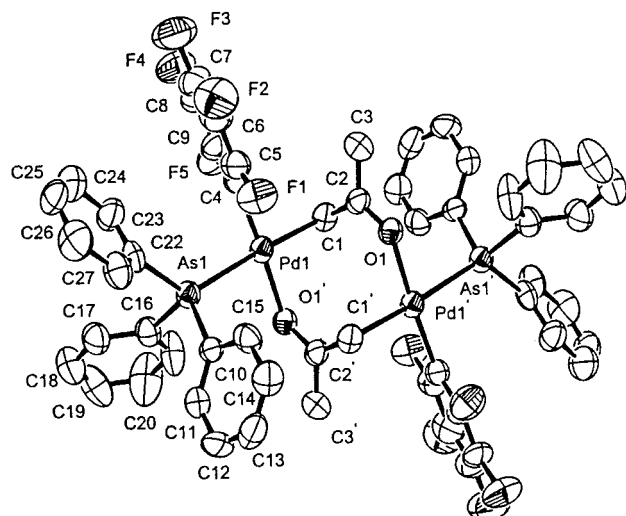


Figure 3. ORTEP diagram of **3**. Thermal ellipsoids are at 50% probability.

Table 1. Selected Bond Distances (Å) and Bond Angles (deg) for Complex 3^a

bond distances		bond angles	
Pd(1)–As(1)	2.4182(14)	C(4)–Pd(1)–O(1)'	176.2(4)
Pd(1)–C(1)	2.106(10)	C(4)–Pd(1)–C(1)	92.7(3)
Pd(1)–C(4)	2.012(11)	O(1)'–Pd(1)–C(1)	89.9(4)
Pd(1)–O(1)'	2.104(7)	C(4)–Pd(1)–As(1)	92.7(3)
Pd(2)–As(2)	2.421(2)	O(1)'–Pd(1)–As(1)	85.2(2)
Pd(2)–C(28)	2.129(11)	C(1)–Pd(1)–As(1)	174.7(3)
Pd(2)–C(31)	2.009(12)	C(31)–Pd(2)–O(2)''	176.3(5)
Pd(2)–O(2)''	2.092(8)	C(31)–Pd(2)–C(28)	90.8(5)
		O(2)''–Pd(2)–C(28)	89.4(4)
		C(31)–Pd(2)–As(2)	94.1(4)
		O(2)''–Pd(2)–As(2)	85.8(2)
		C(28)–Pd(2)–As(2)	175.1(3)

^a Symmetry transformations used to generate equivalent atoms: ' $-x, -y+2, -z$ '' $-x, -y, -z+1$.

The palladium–carbon bond lengths in this complex (2.162(10) and 2.137(10) Å) are just slightly longer than those noted for **3** (2.106(10) and 2.130(11) Å). The

palladium–oxygen bond lengths in **3** (2.104(7) and 2.092(8) Å) are similar to those in the previously studied species (2.116(5) and 2.101(5) Å). The lengths of the carbon–oxygen double bonds in **3** (1.285(12) and 1.248(14) Å) are surprisingly dissimilar for no obvious reason and bracket those for the previously studied $\{\text{CH}_2\text{C}(\text{Ph})=\text{O}\}$ derivative (1.261(12) and 1.256(10) Å). There was also some evidence for the dissociation of the $\{\text{CH}_2\text{C}(\text{Ph})=\text{O}\}$ complex in solution.

Monomeric Acetyl Palladium Complexes $[(\text{AsPh}_3)(\text{C}_6\text{F}_5)\text{Pd}\{\text{CH}_2\text{C}(\text{O})\text{CH}_3\}(\text{t-BuNC})]$ and $[(o\text{-C}_6\text{H}_4\text{CH}_2\text{NMe}_2)\text{Pd}\{\text{CH}_2\text{C}(\text{O})\text{Me}\}(\text{t-BuNC})]$. The reactions of **2** and **3** with *t*-BuNC (in 1:1 molar ratio) in benzene or dichloromethane at room temperature yield the monomeric complexes $[(o\text{-C}_6\text{H}_4\text{CH}_2\text{NMe}_2)\text{Pd}\{\text{CH}_2\text{C}(\text{O})\text{Me}\}(\text{CNBu-}t)]$ **4** and **5**, respectively (Schemes 2 and 5). The insertion of *t*-BuNC into the Pd–C bond of $[(\text{PPh}_3)_2(\text{Cl})\text{Pd}\{\text{CH}_2\text{C}(\text{O})\text{Ph}\}]$ to yield *trans*- $[(\text{PPh}_3)_2(\text{Cl})\text{PdC}(\text{NHBu-}t)=\text{CH}-\text{C}(\text{O})\text{Ph}]$ and the reaction of $[(o\text{-C}_6\text{H}_4\text{CH}_2\text{NMe}_2)\text{PdCl}(\text{CNBu-}t)]$ with *t*-BuNC to give the iminoacyl complex $[(o\text{-C}_6\text{H}_4(\text{C}=\text{NR})\text{CH}_2\text{NMe}_2)\text{PdCl}(\text{CNBu-}t)]$ have been previously reported.^{11,41} The IR spectrum of **4** shows a $\nu(\text{CN})$ absorption⁴² at 2182 (2200 for **5**) cm^{-1} and a $\nu(\text{CO})$ band at 1638 (1650 for **5**) cm^{-1} . These last values are similar to those found in the related monomeric β -carbonylmethyl palladium complexes^{9–11,43–45} and are indicative of the absence of interaction between the carbonyl group and the palladium atom. The singlet signals observed in the ^1H NMR spectrum of **4** at δ 2.60 (2.81 for **5**) and 2.14 (2.06 for **5**) are assignable to the methylene and methyl protons of the acetyl ligand, respectively. Further, a unique singlet resonance for the N-Me groups and a singlet resonance for the CH_2 protons of bonded $\text{C}_6\text{H}_4\text{-CH}_2\text{NMe}_2$ are observed. In accord with the structure of the starting dimer **3**, a MeCOCH_2 -*trans*-to- NMe_2 ligand geometry for monomer **4** is proposed. Proton NOE difference spectra confirmed this suggestion.

(40) Forniés, J.; Navarro, R.; Tomás, M.; Urriolabeitia, E. P. *Organometallics* **1993**, *12*, 940.

(41) Yamamoto, Y.; Yamazaki, H. *Inorg. Chim. Acta* **1980**, *41*, 229.

(42) Ruiz, J.; M. T. Martínez; Vicente, C.; García, G.; López, G.; Chaloner, P. A.; Hitchcock, P. B. *Organometallics* **1993**, *12*, 1594.

(43) Fuchita, Y.; Harada, Y. *Inorg. Chim. Acta* **1993**, *208*, 43.

(44) Suzuki, K.; Yamamoto, H. *Inorg. Chim. Acta* **1993**, *208*, 225.

(45) Allan, D. R.; Clark, S. J.; Ibberson, R. M.; Parsons, S.; Pulham, C. R.; Sawyer, L. *Chem. Commun.* **1999**, 751–752.

(37) Suzuki, H.; Moro-Oka, Y.; Ikawa, T.; Miyajima, T.; Tanaka, I.; Ashida, T. *Chem. Lett.* **1982**, 1369.

(38) García-Ruano, J. L.; González, A. M.; López-Solera, I.; Masaguer, J. R.; Navarro-Ranninger, C.; Raithby, P. R.; Rodríguez, J. H. *Angew. Chem., Int. Ed. Engl.* **1995**, *34*, 1351.

(39) Yamaguchi, T.; Sasaki, Y.; Ito, T. *J. Am. Chem. Soc.* **1990**, *112*, 4038.

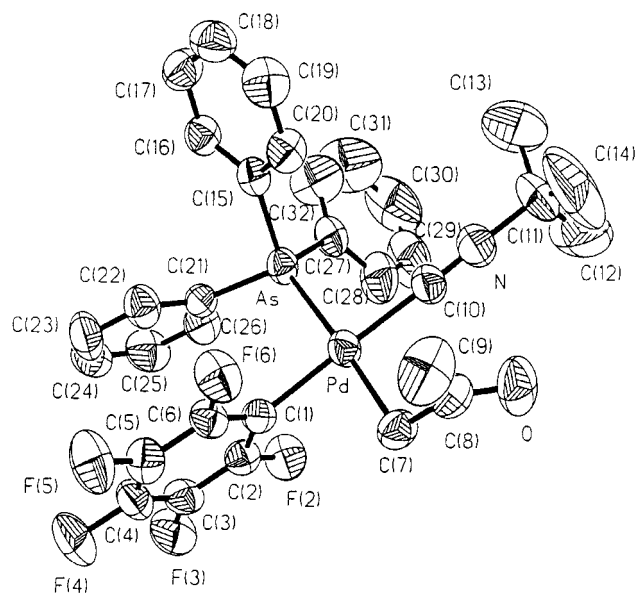


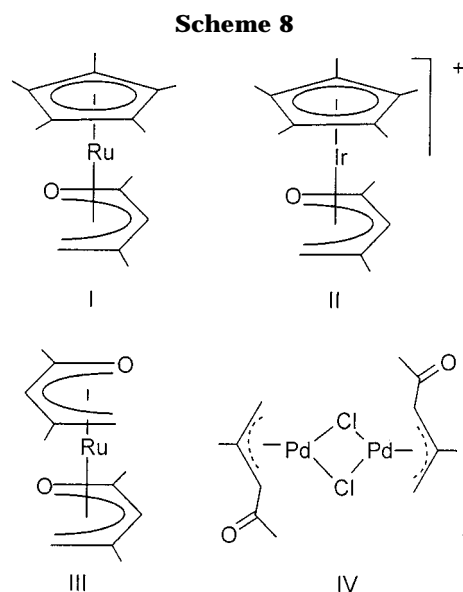
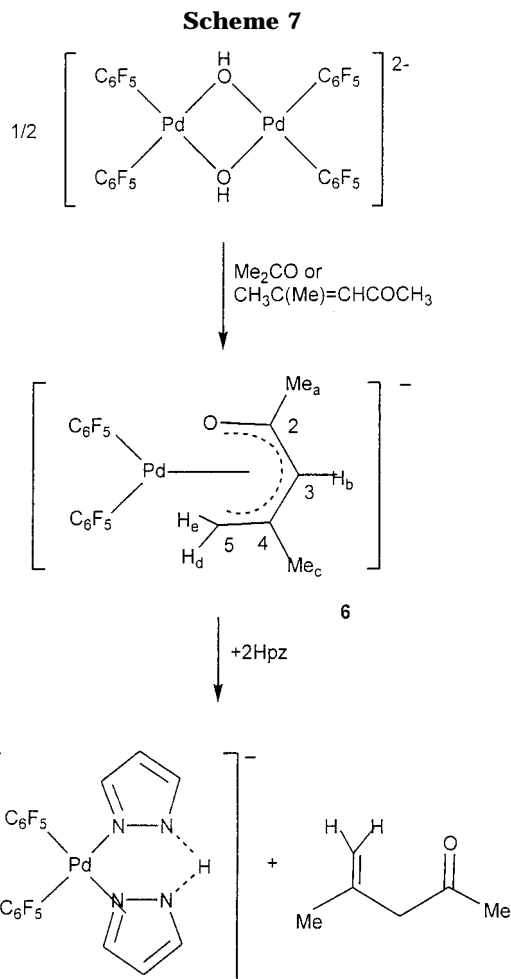
Figure 4. ORTEP diagram of **5**. Thermal ellipsoids are at 50% probability.

Table 2. Selected Bond Distances (Å) and Bond Angles (deg) for Complex 5

bond distances		bond angles	
Pd–C(10)	1.971(4)	C(10)–Pd–C(1)	178.8(2)
Pd–C(1)	2.035(4)	C(10)–Pd–C(7)	91.9(2)
Pd–C(7)	2.111(4)	C(1)–Pd–C(7)	86.8(2)
Pd–As	2.4393(5)	C(10)–Pd–As	91.39(11)
O–C(8)	1.230(5)	C(1)–Pd–As	89.84(10)
C(7)–C(8)	1.435(5)	C(7)–Pd–As	176.59(11)
C(8)–C(9)	1.493(6)		

The crystal structure of **5** has been established by X-ray diffraction. A view of complex **5** is given in Figure 4, and Table 2 lists some selected bond lengths and bond angles. The geometry around the metal atom is essentially square planar; the deviation of Pd from the best plane through the atoms defining the coordination plane is 0.008(2) Å. The distances Pd–As and Pd–C(7) are similar to that found in the μ -acetyl complex **3**. The length of the carbon–oxygen double bond (1.230(5) Å) is shorter than that found in the bridged complex **3** but longer than that of the solid acetone.⁴⁶ The distances C–CH₂ and C–CH₃ are shortened and enlarged respectively with regard to those of the solid acetone.⁴⁶ The enolate ligand is nearly perpendicular to the mean coordination plane (dihedral angle 79.4(3)°); this conformation is found in [Pt(CH₂COCH₃)Cl(bipy)]⁴⁷ or in [Pd(CH₂COPh)Cl(PPh₃)₂].¹¹ The Pd–C10 distance, 1.971(4) Å, is inside the range of distances found for isocyanide complexes of palladium.⁴⁸

2,4-Dimethyl-1-oxapenta-1,3-dienylpalladium Complex [NBu₄][(C₆F₅)₂Pd(μ ⁵-2,4-Me₂-C₄H₃O)]. When a solution of the di- μ -hydroxo palladium complex [NBu₄]₂[(C₆F₅)₂Pd(μ -OH)₂(C₆F₅)₂] in acetone was heated under reflux for 6 h, the 1-oxapenta-1,3-dienylpalladium complex **6** was obtained (Scheme 7). A metal-catalyzed aldol condensation is perhaps involved in the formation



of the oxodienyl ligand. Alternatively, complex **6** can also be prepared from mesityl oxide (Scheme 7). The related ruthenium complex [Cp**Ru*(η ⁵-2,4-Me₂-C₄H₃O)] (**I**, Scheme 8) has been previously reported using [Cp**Ru*Cl]₄ and mesityl oxide [CH₃C(Me)=CHCOCH₃] in the presence of the mild base K₂CO₃ in hot THF.⁴⁹ The reaction of coordinated acetone solvent species with acetone to

(46) Falvello, L. R.; Garde, R.; Miqueleiz, E. M.; Tomás, M.; Urriolabeitia, E. P.; *Inorg. Chim. Acta* **1997**, 264, 297–303.

(47) Orpen, A. G.; Brammer, L.; Allen, F. H.; Kennard, O.; Watson, D. G.; Taylor, R. *J. Chem. Soc., Dalton Trans.* **1989**, S1.

(48) Suzuki, K.; Jindo, A.; Hanaki, K. *Inorg. Chim. Acta* **1993**, 210, 57.

(49) Trakarnpruk, W.; Ariff, A. M.; Ernst, R. D. *Organometallics* **1992**, 11, 1686.

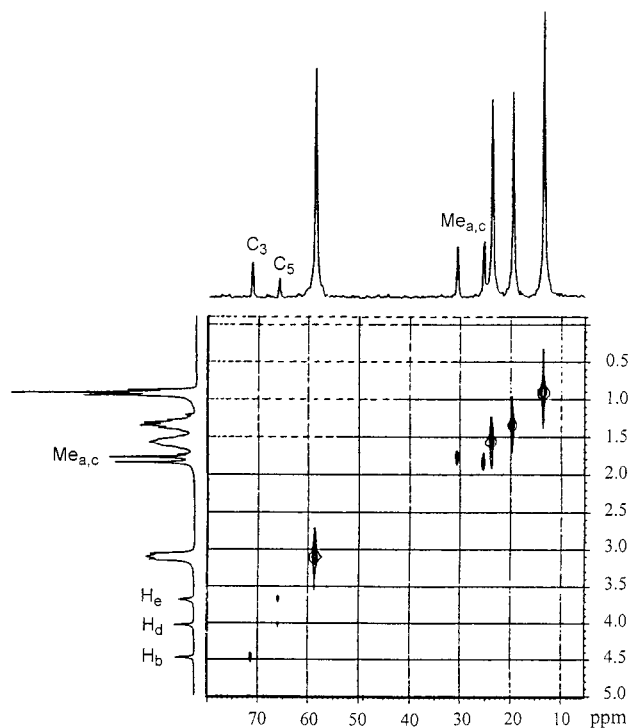
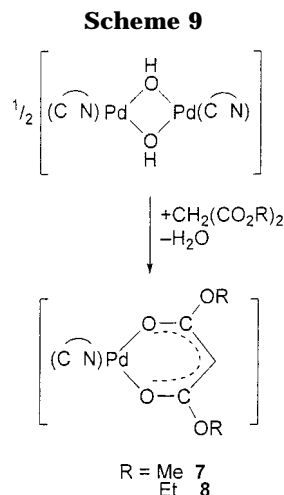


Figure 5. ^1H – ^{13}C COSY of **6**.

give the analogous iridium cation $[\text{Cp}^*\text{Ir}(\eta^5\text{-}2,4\text{-Me}_2\text{-C}_4\text{H}_3\text{O})]^+$ (**II**, Scheme 8) has also been previously reported by Maitlis et al.⁵⁰ The crystal structures of the ruthenium complexes $[\text{Ru}(\eta^5\text{-}2,4\text{-Me}_2\text{-C}_4\text{H}_3\text{O})_2]$ (**III**, Scheme 8) and $[\text{Cp}^*\text{Ru}(\eta^5\text{-}3,5\text{-Me}_2\text{-C}_4\text{H}_3\text{O})]$ have been reported.^{49,51} On the other hand, the deprotonation of mesityl oxide to form the η^3 -allylpalladium complex $[\text{C}_6\text{H}_5\text{O-PdCl}]_2$ (**IV**, Scheme 8) is well established,⁵² and its characterization was based mainly on the observation of $\nu(\text{CO})$ at 1690 cm^{-1} , suggesting that the carbonyl oxygen was not coordinated and, therefore, the mode of bonding was η^3 . However, the IR spectrum of the bis-(pentafluorophenyl) complex **6** shows a strong, broad absorption at 1635 cm^{-1} assigned to coordinated carbonyl, indicating that the η^3 -allyl mode of bonding should be discarded. It also shows the characteristic absorptions of the C_6F_5 group³³ and a split band at ca. 800 cm^{-1} assigned to the *cis*-Pd(C_6F_5)₂ moiety.^{34,53} The ^{19}F NMR spectrum of **6** reveals the presence of two different types of C_6F_5 groups, one *trans* to C and one *trans* to O. Each freely rotating pentafluorophenyl ring gives three resonances (in the ratio 2:2:1) for the *ortho*-, *meta*-, and *para*-fluorine atoms, respectively. The assignment of signals (see Experimental Section) and the structure was performed using a ^1H and ^{13}C NMR study, which comprised heteronuclear (^1H – ^{13}C) COSY experiments and proton NOE differential spectra. Thus COSY experiments show (see Figure 5 and Scheme 7 for numbering) that the ^1H signals at 3.98 (s, H_d) and 3.65 (s, H_e) are correlated with the ^{13}C signal at 65.7 ppm (C(5)), and the ^1H resonance at 4.45 (s, H_b) is correlated with the ^{13}C signal at 71.1 ppm. On the other hand,



proton NOE difference spectra show that irradiation of the CH signal at δ 4.45 produces an enhancement of the methyl signals at 1.82 and 1.74. The same effect has been found in the related complex $[\text{NBu}_4][(\text{C}_6\text{F}_5)_2\text{-Pd}(\text{acetylacetonate})]$.²⁹ The ^{13}C NMR signal observed at δ 197.1, assigned to the CO resonance, is in the region of the corresponding resonance for the related acetylacetonate complex cited above (δ 185.8). Unfortunately no suitable single crystals for X-ray diffraction were obtained. The reaction of **6** with the weak acid pyrazole (Hpz) yields (**Scheme 7**) the previously reported pyrazole–pyrazolate complex $[\text{NBu}_4][(\text{C}_6\text{F}_5)_2\text{Pd}(\text{pz})(\text{Hpz})]$ together with 4-methyl-4-penten-2-one;⁵⁴ no mesityl oxide was detected by ^1H NMR, although the acid-catalyzed double-bond migration in the former ketone toward the latter has been previously described.^{30,55}

Dialkylmalonate Palladium Complex [(*o*-C₆H₄CH₂NMe₂)Pd{*O,O'*-CH(CO₂R)₂}]. The reaction (1:2) of $[\{(o\text{-C}_6\text{H}_4\text{CH}_2\text{NMe}_2)\text{Pd}\}_2(\mu\text{-OH})_2]$ with $\text{CH}_2(\text{CO}_2\text{R})_2$ (R = Me, Et) leads (Scheme 9) to the dialkyl malonate palladium complexes $[(o\text{-C}_6\text{H}_4\text{CH}_2\text{NMe}_2)\text{Pd}\{O,O'\text{-CH}(\text{CO}_2\text{R})_2\}]$ (**7**, R = Me; **8**, R = Et). Dialkyl malonates are very versatile ligands, exhibiting either *C*- or *O,O'*-bonding modes due to their small degree of enolization and depending, in part, on the particular metal ion.^{56,57} The IR spectra of complexes **7** and **8** show a strong $\nu(\text{CO})$ absorption at ca. 1620 cm^{-1} which excludes the presence of the *C*-bonding mode.^{57,58} The unique singlet resonances observed in the ^1H NMR spectra for the CH_2N and NMe_2 protons show that the molecular plane of complexes **7** and **8** is a symmetry plane. Moreover, the two different sets of resonances observed for the R substituents of the $\text{CH}(\text{CO}_2\text{R})_2$ ligand (R = Me or Et) are in agreement with the *O,O'*-bonding mode proposed.^{59,60}

The molecular structure of **8** (crystals obtained by slow diffusion of *n*-hexane into a CH_2Cl_2 solution of **8**

(50) White, C.; Thompson, J.; Maitlis, P. M. *J. Organomet. Chem.* **1977**, *134*, 319.

(51) Schmidt, T.; Goddard, R. *J. Chem. Soc., Chem. Commun.* **1991**, 1427.

(52) Parshall, G. W.; Wilkinson, G. *Inorg. Chem.* **1962**, *1*, 896.

(53) Alonso, E.; Forniés, J.; Fortuño, C.; Tomás, M. *J. Chem. Soc., Dalton Trans.* **1995**, 3777.

(54) López, G.; Ruiz, J.; Vicente, C.; Martí, J. M.; García, G.; Chaloner, P. A.; Hitchcock, P. B.; Harrison, R. M. *Organometallics* **1992**, *11*, 4091.

(55) Noyce, D. S.; Evett, M. *J. Org. Chem.* **1972**, *37*, 397.

(56) Newkome, G. R.; Gupta, V. K. *Inorg. Chim. Acta* **1982**, *65*, L165.

(57) Newkome, G. R.; Gupta, V. K.; Taylor, H. C. R., Fronczek, F. *Organometallics* **1984**, *3*, 1549.

(58) Ito, T.; Yamamoto, A. *J. Organomet. Chem.* **1979**, *174*, 237.

(59) Chung, P. J.; Suzuki, H.; Moro-oka, Y.; Ikawa, T. *Chem. Lett.* **1980**, 63.

(60) Sugimoto, R.; Eikawa, H.; Suzuki, H.; Moro-oka, Y.; Ikawa, T. *Bull. Chem. Soc. Jpn.* **1981**, *54*, 2849.

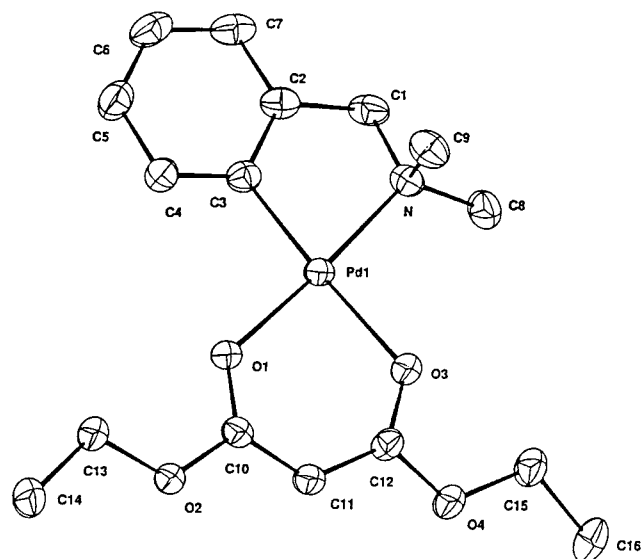


Figure 6. ORTEP diagram of **8**. Thermal ellipsoids are at 50% probability.

Table 3. Selected Bond Distances (Å) and Bond Angles (deg) for Complex 8

Bond Distances		Bond Angles	
Pd–C(3)	1.961(3)	C(3)–Pd–O(1)	93.31(10)
Pd–O(1)	2.030(2)	C(3)–Pd–N	82.47(11)
Pd–N	2.047(2)	O(1)–Pd–N	174.83(8)
Pd–O(3)	2.102(2)	C(3)–Pd–O(3)	175.83(10)
		O(1)–Pd–O(3)	90.35(8)
		N–Pd–O(3)	93.97(9)

at room temperature) provides further characterization. The structure of **8** is shown in Figure 6. Selected bond distances and bond angles are given in Table 3. Coordination at palladium is approximately square planar, although the angles around palladium deviate from 90° due to the bite of the cyclometalated ligand. The C(3)–Pd–N angle of 82.47(11)° is within the normal range for such complexes.^{61–64} The palladium–carbon bond length is at the low end of the range of those reported for the carbon *trans* to oxygen, and the palladium–nitrogen distance is also shorter than most of those reported for comparable species.^{61–74} The five-membered

(61) Matt, D.; Guillemin, J.-C.; Ziesel, R.; Balegroune, F.; Grandjean, D. *Acta Crystallogr., Sect. C* **1994**, *50*, 193.

(62) Fallon, G. D.; Gatehouse, B. M. *J. Chem. Soc., Dalton Trans.* **1974**, 1632.

(63) Narayan, S.; Jain, V. K.; Butcher, R. J. *J. Organomet. Chem.* **1997**, *549*, 73.

(64) Barr, N.; Dyke, S. F.; Smith, G.; Kennard, C. H. L.; McKee, V. *J. Organomet. Chem.* **1985**, *288*, 109.

(65) Andrieu, J.; Braunstein, P.; Drillon, M.; Dusausoy, Y.; Ingold, F.; Rabu, P.; Tiripicchio, A.; Ugozzoli, F. *Inorg. Chem.* **1996**, *35*, 5986.

(66) Andrieu, J.; Braunstein, P.; Dusausoy, Y.; Ghermani, N. E. *Inorg. Chem.* **1996**, *35*, 7174.

(67) Bouaoud, S. E.; Braunstein, P.; Grandjean, D.; Matt, D.; Nobel, D. *J. Chem. Soc., Chem. Commun.* **1987**, 488.

(68) Russell, D. R.; Tucker, P. A. *J. Chem. Soc., Dalton Trans.* **1975**, 1743.

(69) Bhattacharyya, P.; Slawin, A. M. Z. Smith, M. B. *J. Chem. Soc., Dalton Trans.* **1998**, 2467.

(70) Ruiz, J.; Cutillas, N.; Sanpedro, J.; López, G.; Hermoso, J. A.; Martínez-Ripoll, M. *J. Organomet. Chem.* **1996**, *526*, 67.

(71) Alsters, P.; Teunissen, H. T.; Boersma, J.; Soek, A. L.; Van Koten, G. *Organometallics* **1993**, *12*, 4691.

(72) Braunstein, P.; Matt, D.; Nobel, D.; Bouaoud, S.-E.; Grandjean, D. *J. Organomet. Chem.* **1986**, *301*, 401.

(73) Braunstein, P.; Matt, D.; Dusausoy, Y.; Fischer, J.; Mitschler, A.; Ricard, L. *J. Am. Chem. Soc.* **1981**, *103*, 5115.

(74) Zhou, Y.; Wagner, B.; Polborn, K.; Sünkel, K.; Beck, W. Z. *Naturforsch.* **1994**, *49b*, 1193.

ring adopts an envelope conformation with the CH₂ group significantly out of the plane.^{65,66} The differences in the Pd–O distances (Pd–O(1) 2.030(2) Å, Pd–O(3) 2.102(2) Å) are in accord with the lower *trans*-influence of the NMe₂ group. Relatively few malonate complexes have been characterized crystallographically, and there are no palladium complexes among them. In **8** the chelating ring of the malonate ligand is close to planar, with a bite angle of 90.35(8)° at palladium. The carbon–carbon bond lengths in the ring (1.388(4) and 1.398(4) Å) show significant double-bond character and indicate almost total delocalization. They are comparable with the related bond lengths in [Ni(α-Np)(PPh₃){CH(COOEt)₂}] (1.396(14) and 1.381(13) Å)⁷⁵ or [Mo(H)(dppf)₂{CH(COOEt)₂}] (1.3865(5) Å).⁷⁶ By contrast, complexes of nondeprotonated malonate esters such as [TiCl₄{CH(COOEt)₂}]⁷⁷ and [VOCl₂{CH(COOEt)₂}]₄⁷⁸ have shorter C–O bond lengths and longer C–C bond lengths in the chelate ring, and the chelate rings are not planar.

Conclusions

The work described herein shows that the hydroxo complexes of the type [(X)(Y)Pd(μ-OH)₂Pd(X)(Y)] are convenient starting reagents for the preparation of bridging C,O-enolato complexes via the acid–base reaction >Pd(μ-OH)₂Pd< + 2 CH₃COCH₃ → >Pd{μ-CH₂C(O)CH₃}₂Pd< + 2H₂O, the outcome being dependent on the identity of the ancillary ligands (X, Y). With the (AsPh₃)(C₆F₅)Pd moiety no reaction takes place, although the bis(μ-enolato) complex is obtained by reacting the corresponding bis(μ-chloro) complex with enolate generated in situ. With the (C–N)Pd moiety both the (μ-OH)(μ-enolato) and bis(μ-enolato) complexes are obtained by reaction between the bis(μ-hydroxo) complex and acetone. However the ligand resulting from aldol condensation is obtained when Pd(C₆F₅)₂ is used. There is a correlation between the reactivity and the basic character of the bis(μ-hydroxo) complex which increases in the order [(AsPh₃)(C₆F₅)Pd(μ-OH)₂Pd(AsPh₃)(C₆F₅)] < [(C–N)Pd(μ-OH)₂Pd(C–N)] < [(C₆F₅)₂Pd(μ-OH)₂Pd(C₆F₅)₂]²⁻, which is in agreement with the order followed by the high-field proton resonance of the μ-OH in the above hydroxo complexes (δ –1.49, –2.40, and –2.84, respectively).⁷⁹

The protonation of the binuclear hydroxo complex by acetone should give an aqua complex intermediate, which we have not been able to detect. However, we have recently reported⁸⁰ the formation of the diaqua complex [(AsPh₃)(C₆F₅)Pd(OH₂)₂](CF₃SO₃) when the corresponding di-μ-hydroxo complex is protonated by triflic acid. The noncoordinating triflate anion facilitates the formation of the aqua complex.

The more basic [(C₆F₅)₂Pd(μ-OH)₂Pd(C₆F₅)₂]²⁻ generates enough enolate for the aldol condensation to

(75) Agnès, G.; Bart, J. C. J.; Calcaterra, M.; Cavigioto, W.; Santini, C. *Transition Met. Chem.* **1986**, *11*, 246.

(76) Minato, M.; Kurishima, M.; Nagai, K.; Yamasaki, M.; Ito, T. *Chem. Lett.* **1994**, 2339.

(77) Sobota, P.; Szafert, S.; Lis, T. *J. Organomet. Chem.* **1993**, *443*, 85.

(78) Sobota, P.; Ejfler, J.; Szafert, S.; Glowiak, T.; Fritzky, I. O.; Szczegot, K. *J. Chem. Soc., Dalton Trans.* **1995**, 1727.

(79) López, G.; García, G.; Ruiz, J.; Sánchez, G.; García, J.; Vicente, C. *J. Chem. Soc., Chem. Commun.* **1989**, 1045.

(80) Ruiz, J.; Florenciano, F.; Vicente, C.; Ramírez de Arellano, M. C.; López, G. *Inorg. Chem. Commun.* **2000**, *3*, 73.

proceed, and the resulting β -hydroxy ketone is dehydrated during the course of the reaction, yielding complex **6**. This reaction resembles the $[(C_6F_5)_2Pd(\mu-OH)_2Pd(C_6F_5)_2]^{2-}$ -catalyzed cyclotrimerization of malonitrile very closely, in which the α -carbon of one malonitrile anion adds to the CN carbon of malonitrile. In this case, a bridging C,N-bound malonitrile complex was isolated.⁸¹

Experimental Section

Instrumental Measurements. C, H, and N analyses were performed with a Carlo Erba model EA 1108 microanalyzer. Decomposition temperatures were determined with a Mettler TG-50 thermobalance at a heating rate of 5 °C min⁻¹ with the solid samples under nitrogen flow (100 mL min⁻¹). Molar conductivities were measured in acetone solution ($c \approx 5 \times 10^{-4}$ mol L⁻¹) with a Crison 525 conductimeter. The NMR spectra were recorded on a Bruker AC 200E or Varian Unity 300 spectrometer, using SiMe₄ and CFCl₃ as the standard, respectively. Infrared spectra were recorded on a Perkin-Elmer 1430 spectrophotometer using Nujol mulls between polyethylene sheets. Mass spectra (positive-ion FAB) were recorded on a V.G. AutoSpecE spectrometer and measured using 3-nitrobenzyl alcohol as the dispersing matrix.

Materials. The starting complexes $[(o-C_6H_4CH_2NMe_2)Pd(\mu-OH)_2]$ (C,N = $o-C_6H_4CH_2NMe_2$),²⁸ $[(AsPh_3)(C_6F_5)Pd(\mu-Cl)_2]$,⁸² and $[NBu_4]_2[(C_6F_5)_2Pd(\mu-OH)_2Pd(C_6F_5)_2]$ ²⁹ were prepared by procedures described elsewhere. Solvents were dried by the usual methods.

Preparation of Complex $[(o-C_6H_4CH_2NMe_2)Pd]_2(\mu-OH)\{\mu-CH_2C(O)CH_3\}$ (1). A suspension of $[(o-C_6H_4CH_2NMe_2)Pd(\mu-OH)_2]$ (60 mg, 0.116 mmol) in acetone (9 mL) was boiled under reflux for 30 min until the starting product was completely dissolved. The resulting solution was then concentrated under vacuum. The addition of hexane caused the precipitation of a white solid, which was collected by filtration and air-dried. Yield: 35%. Anal. Calcd for C₂₁H₃₀N₂O₂Pd₂: C, 45.4; H, 5.5; N, 5.0. Found: C, 45.7; H, 5.6; N, 4.9. Mp: 147 °C dec. IR (Nujol, cm⁻¹): $\nu(OH)$, 3560; $\nu(CO)$, 1564, 1556. ¹H NMR (CDCl₃): δ 7.3–6.9 (m, 8 H, aromatics), 3.84 (s, 2 H, NCH₂), 3.81 (s, 2 H, NCH₂), 3.22 (s, 2 H, CH₂CO), 2.74 (s, 6 H, NMe₂), 2.67 (s, 6 H, NMe₂), 2.24 (s, 3 H, CH₃CO), -2.01 (s, 1 H, OH). ¹³C{¹H} NMR (CDCl₃): δ 148.5, 147.6, 147.5, 144.2 (aromatics C), 135.2, 130.7, 125.3, 124.6, 124.0, 123.0, 122.0, 121.4 (aromatics CH), 72.8 (CH₂NMe₂), 71.5 (CH₂NMe₂), 51.7 (NMe₂), 50.1 (NMe₂), 41.6 (CH₂CO), 28.7 (CH₃CO). Positive-ion FAB mass spectrum: m/z 556 (M - O)⁺.

Preparation of Complex $[(o-C_6H_4CH_2NMe_2)Pd]_2(\mu-CH_2C(O)CH_3)_2$ (2). A suspension of $[(o-C_6H_4CH_2NMe_2)Pd(\mu-OH)_2]$ (60 mg, mmol) in acetone (4 mL) was boiled under reflux for 4 h. The resulting precipitate was collected by filtration, washed with hexane, and air-dried. Yield: 74%. Anal. Calcd for C₂₄H₃₄N₂O₂Pd₂: C, 48.4; H, 5.8; N, 4.7. Found: C, 48.4; H, 5.7; N, 4.6. Mp: 186 °C dec. IR (Nujol, cm⁻¹): $\nu(CO)$, 1566. ¹H NMR at 25 °C (CDCl₃): δ 6.9 (br, 8 H, aromatics) 4.1 (br, 2 H, NCH₂), 3.6–3.5 (br, 4 H, NCH₂ + CH₂CO), 2.6 (br, 20 H, CH₂CO + CH₃CO + NMe₂). ¹H NMR at -20 °C (CDCl₃): δ 6.8 (m, 8 H, aromatics) 4.13 (d, 2 H, NCH₂, J 13.8), 3.60 (d, 2 H, NCH₂, J 13.8), 3.53 (s, 2 H, CH₂CO), 2.73 (s, 2 H, CH₂CO), 2.65 (s, 6 H, NMe₂), 2.63 (s, 6 H, CH₃CO), 2.17 (s, 6 H, NMe₂). ¹³C{¹H} NMR at -20 °C (CDCl₃): δ 148.9, 145.5 (aromatics C), 134.0, 125.3, 123.5, 122.4 (aromatics CH), 71.2 (CH₂NMe₂), 51.0 (NMe₂), 50.4 (NMe₂), 33.4 (CH₂CO), 31.4 (CH₃CO).

Preparation of Complex $[(AsPh_3)(C_6F_5)Pd]_2(\mu-CH_2C(O)CH_3)_2$ (3). To a suspension of $[(Pd(C_6F_5)(AsPh_3)(\mu-Cl)_2]$ (290 mg, 0.236 mmol) in acetone (15 mL) was added 20% $[NBu_4]OH(aq)$ (0.618 mL, 0.472 mmol), and the resulting solution was stirred at room temperature for 30 min and then solvent was partially evaporated under reduced pressure. On addition of methanol and a few drops of water, a pale yellow solid precipitated, which was filtered off and air-dried. The solid was redissolved in CH₂Cl₂ and then filtered through a small column packed with Florisil. The filtrate was concentrated to dryness. Addition of ether/hexane to the residue followed by vigorous stirring rendered a pale yellow suspension, from which a pale yellow solid was collected by filtration and air-dried. Complex **3** was recrystallized from dry toluene/hexane. Yield: 83%. Anal. Calcd for C₅₄H₄₀As₂F₁₀O₂Pd₂: C, 50.9; H, 3.2. Found: C, 50.3; H, 3.1. Mp: 166 °C dec. IR (Nujol, cm⁻¹): $\nu(CO)$, 1538 Pd-C₆F₅ str, 784. ¹H NMR at 25 °C (CDCl₃): δ 7.30 (m, AsPh₃), 3.67 (br, CH₂CO), 3.31 (br, CH₂CO), 2.69 (br, CH₂CO), 2.56 (br, CH₂CO), 1.87 (br, CH₃CO), 0.99 (br, CH₃CO). ¹H NMR at -20 °C (CDCl₃): δ 7.30(m, AsPh₃), 3.70 (s, CH₂CO), 3.35 (d, CH₂CO, J = 3.2 Hz), 2.70 (s, CH₂CO), 2.62 (d, CH₂CO, J = 3.2 Hz), 1.91 (s, CH₃CO), 1.02 (s, CH₃CO). ¹⁹F NMR at 25 °C: δ -115.8 (m, F_o), -116.8 (d, F_o, J_{om} = 22.6 Hz), -117.8 (d, F_o, J_{om} = 22.6 Hz), -161.7 (t, F_p, J_{pm} = 20.3 Hz), -162.5 (t, F_p, J_{pm} = 20.3 Hz), -163.3 (m, F_m), -163.7 (m, F_m), -164.1 (m, F_m).

Preparation of Complex $[(o-C_6H_4CH_2NMe_2)Pd](CH_2C(O)Me)(t-BuNC)$ (4). To a suspension of complex **2** (80 mg, 0.134 mmol) in benzene (2 mL) was added *t*-BuNC (30 μ L, 0.268 mmol). The resulting solution was stirred at room temperature for 5 min, and the solvent was then removed under vacuum. The residue was treated with hexane, and an orange solid was collected by filtration and air-dried. The solid was kept in a refrigerator at 5 °C. Yield: 55%. Anal. Calcd for C₁₇H₂₆N₂O₁Pd: C, 53.6; H, 6.8; N, 7.4. Found: C, 53.5; H, 6.9; N, 7.3. Mp: 103 °C dec. IR (Nujol, cm⁻¹): $\nu(CN)$, 2182; $\nu(CO)$, 1638. ¹H NMR (CDCl₃): δ 7.1–6.9 (m, 4 H, aromatics), 3.85 (s, 2 H, NCH₂), 2.72 (s, 6 H, NMe₂), 2.60 (s, 2 H, CH₂CO), 2.14 (s, 3 H, CH₃CO). Positive-ion FAB mass spectrum: m/z 381 (M + 1)⁺, 324 (M + 1 - CH₂COCH₃)⁺.

Preparation of Complex $[(AsPh_3)(C_6F_5)Pd](CH_2C(O)CH_3)(t-BuNC)$ (5). To a solution of complex **3** (90 mg, 0.07 mmol) in CH₂Cl₂ (6 mL) was added *t*-BuNC (15.8 μ L, 0.14 mmol). The resulting solution was stirred at room temperature for 15 min and concentrated under vacuum. The addition of hexane caused the precipitation of a white solid, which was collected by filtration, washed with hexane, and air-dried. Yield: 70%. Anal. Found: C, 53.2; H, 4.0; N, 1.9. Calcd for C₃₂H₂₉F₅NOAsPd: C, 53.4; H, 4.0; N, 2.0. IR (Nujol, cm⁻¹): $\nu(CN)$, 2204; $\nu(CO)$, 1650; Pd-C₆F₅ str, 784. ¹H NMR: δ 7.60–7.34 (15 H, AsPh₃), 2.81 (s, 2 H, CH₂), 2.06 (s, 3 H, CH₃CO), 1.20 (s, 9 H, CH₃, *t*-BuNC). ¹⁹F NMR: δ -116.2 (d, F_o, J_{om} = 22.6 Hz), -162.5 (t, F_p, J_{pm} = 20.3 Hz), -163.8 (m, F_m).

Preparation of Complex $[NBu_4][(C_6F_5)_2Pd(\eta^5-2,4-Me_2-C_4H_5O)]$ (6). A solution of $[NBu_4]_2[(C_6F_5)_2Pd(\mu-OH)_2Pd(C_6F_5)_2]$ in acetone (15 mL) was heated under reflux with stirring for 6 h, and the solvent was then removed in vacuo. The residue was treated with hexane to remove any traces of solvent and then evaporated to dryness. This was repeated several times until a white solid was filtered off and air-dried. Yield: 78%.

Alternatively, mesityl oxide [CH₃C(Me)=CHCOCH₃] (0.488 mmol) was added to a solution of $[NBu_4]_2[(C_6F_5)_2Pd(\mu-OH)_2Pd(C_6F_5)_2]$ (0.1 g, 0.0714 mmol) in toluene (8 cm³); the solution was heated under reflux with stirring for 6 h, and the solvent was then removed in vacuo. The residue was treated with hexane to remove any traces of mesityl oxide and then evaporated to dryness. This was repeated several times. Addition of 2-propanol/hexane afforded a white solid, which was filtered off and air-dried. Yield: 80%. Mp: 211 °C dec. Λ_M = 108 Ω^{-1} cm² mol⁻¹. IR (Nujol, cm⁻¹): $\nu(CO)$, 1635; Pd-C₆F₅ str, 780, 765. Anal. Calcd for C₃₄H₄₅NF₁₀OPd: C, 52.35;

(81) Ruiz, J.; Rodríguez, V.; López, G.; Casabó, J.; Molins, E.; Miravittles, C. *Organometallics* **1999**, *18*, 1177.

(82) Usón, R.; Forniés, J.; Navarro, R.; García, M. P. *Inorg. Chim. Acta* **1979**, *33*, 69.

Table 4. Crystal Structure Determination Details

	3	5	8
formula	C ₅₄ H ₄₀ As ₂ F ₁₀ O ₂ Pd ₂	C ₃₂ H ₂₉ AsF ₅ NOPd	C ₁₆ H ₂₃ NO ₄ Pd
fw	1273.5	719.88	399.7
temperature (K)	293(2)	298(2)	293(2)
cryst syst	triclinic	monoclinic	monoclinic
space group	<i>P</i> $\bar{1}$ (no. 2)	<i>P</i> 2 ₁ / <i>n</i> (no. 14)	<i>P</i> 2 ₁ / <i>c</i> (no. 14)
cell dimens			
<i>a</i> (Å)	12.486(3)	11.3502(9)	6.524(2)
<i>b</i> (Å)	14.119(3)	10.5017(7)	13.570(3)
<i>c</i> (Å)	17.022(4)	26.568(2)	19.502(3)
α (deg)	69.19(2)		
β (deg)	70.35(2)	95.973(7)	91.10(2)
γ (deg)	80.13(2)		
cell vol (Å ³)	2637.1(10)	3149.7(4)	1726.2(6)
<i>Z</i>	2	4	4
<i>D</i> _{calc} (g cm ⁻³)	1.60	1.518	1.54
<i>F</i> (000)	1256	1440	816
monochromated Mo Kα	0.71069	0.71069	0.71073
radiation, λ (Å)			
μ (mm ⁻¹)	2.00	1.686	1.09
cryst size (mm)	0.30 × 0.25 × 0.10	0.30 × 0.15 × 0.10	0.4 × 0.4 × 0.3
θ range for data collection (deg)	2 to 25	3.02 to 24.99	2 to 25
index ranges	0 ≤ <i>h</i> ≤ 14, -16 ≤ <i>k</i> ≤ 16, -18 ≤ <i>l</i> ≤ 20	0 ≤ <i>h</i> ≤ 13, -12 ≤ <i>k</i> ≤ 12, -31 ≤ <i>l</i> ≤ 31	0 ≤ <i>h</i> ≤ 7, 0 ≤ <i>k</i> ≤ 16, -23 ≤ <i>l</i> ≤ 23
no. of reflns collected	9254	11 358	3302
ind reflns	9254	5553 [<i>R</i> (int) = 0.0435]	3029 [<i>R</i> (int) = 0.0224]
structure solution	SHELXS-86	SHELXTL-5.0	SHELXS-86
refinement method	full-matrix least-squares on <i>F</i> ² SHELXL-97	full-matrix-block least-squares on <i>F</i> ² SHELXTL-5.0	full-matrix least-squares on <i>F</i> ² SHELXL-97
no. of data/restraints/params	9254/0/631	5553/36/398	3029/0/200
goodness-of-fit on <i>F</i> ²	1.059	1.007	1.027
final <i>R</i> indices [<i>I</i> > 2σ(<i>I</i>)]	<i>R</i> 1 = 0.075, <i>wR</i> 2 = 0.190	<i>R</i> 1 = 0.0372, <i>wR</i> 2 = 0.0614	<i>R</i> 1 = 0.026, <i>wR</i> 2 = 0.071
<i>R</i> indices (all data)	<i>R</i> 1 = 0.140, <i>wR</i> 2 = 0.231	<i>R</i> 1 = 0.0732, <i>wR</i> 2 = 0.0709	<i>R</i> 1 = 0.033, <i>wR</i> 2 = 0.076
largest diff peak and hole (e Å ⁻³)	1.79 and -1.07	0.260 and -0.335	0.42 and -0.64

H, 5.81; N, 1.80. Found: C, 52.12; H, 5.71; N, 1.83. ¹H NMR (CDCl₃): δ 4.45 (s, H_b), 3.98 (s, H_d), 3.65 (s, H_e), 1.82, 1.74 (ss, Me_a, Me_c) and additional peaks from [NBu₄]⁺. ¹³C{¹H} NMR (CDCl₃): δ 197.1 (C(2)), 127.4 (C(4)), 71.1 (C(3)), 65.7 (C(5)), 30.4, 25.3 (Me_a and Me_c) and additional peaks from [NBu₄]⁺. ¹⁹F NMR (CDCl₃): δ -110.8 (d, 2 *F*_o, *J*_{om} 30.5 Hz), -111.5 (d, 2 *F*_o, *J*_{om} 29.1 Hz), -164.0 (t, 1 *F*_p, *J*_{mp} 19.8 Hz), -164.3 (t, 1 *F*_p, *J*_{mp} 19.8 Hz), -165.2 (m, 4 *F*_m).

Reaction of Complex 6 with Pyrazole. To a solution of complex **6** (60 mg, 0.0769 mmol) in CDCl₃ (0.6 mL) was added pyrazole (Hpz) (10.47 mg, 0.1538 mmol). The resulting solution was stirred at room temperature for 30 min, during which time the previously known⁴⁶ pyrazole-pyrazolate complex [NBu₄]₂[(C₆F₅)₂Pd(pz)(Hpz)] precipitated spontaneously, which was filtered off and air-dried. (¹H NMR in Me₂CO-*d*₆: 7.60 (d, 2 H, 5-H), 6.65 (d, 2 H, 3-H), 6.05 (pseudo-t, 2 H, 4-H)). The filtrate was directly studied by ¹H NMR and identified⁴⁷ as 4-methyl-4-penten-2-one. (¹H NMR (CDCl₃): δ 4.91 (br, 1 H), 4.79 (br, 1 H), 3.08 (s, 2 H), 2.12 (s, 3 H), 1.71 (s, 3H)).

Synthesis of Complexes 7 and 8. To a suspension of [(*o*-C₆H₄CH₂NMe₂)Pd(*μ*-OH)]₂ (80 mg, 0.155 mmol) in dichloromethane (5 mL) was added the corresponding dialkyl malonate CH₂(CO₂R)₂ (R = Me, Et) (1.55 mmol). The resulting solution was stirred at room temperature for 1 h, and the solvent was then removed under vacuum. The residue was treated with hexane (R = Me) or hexane/ether (R = Et), and the solid was collected by filtration and air-dried.

Complex 7. Yield: 80%. Anal. Calcd for C₁₄H₁₉N₁O₄Pd₁: C, 45.2; H, 5.2; N, 3.8. Found: C, 45.4; H, 5.3; N, 3.7. Mp: 166 °C dec. IR (Nujol, cm⁻¹): ν(CO), 1620. ¹H NMR (CDCl₃): δ 7.1–

6.8 (m, 4 H, aromatics), 4.20 (s, 1 H, CH(CO₂Me)₂), 3.66 (s, 3 H, CH₃O), 3.54 (s, 3 H, CH₃O), 3.88 (s, 2 H, NCH₂), 2.81 (s, 6 H, NMe₂). Positive-ion FAB mass spectrum: *m/z* 371 (M⁺).

Complex 8. Yield: 75%. Anal. Calcd for C₁₆H₂₃N₁O₄Pd₁: C, 48.1; H, 5.8; N, 3.5. Found: C, 48.2; H, 5.8; N, 3.5. Mp: 161 °C dec. IR (Nujol, cm⁻¹): ν(CO), 1620. ¹H NMR (CDCl₃): δ 7.1–6.9 (m, 4 H, aromatics), 4.24 (s, 1 H, CH(CO₂Et)₂), 4.19 (q, 2 H, CH₂O, *J* 7.1), 4.09 (q, 2 H, CH₂O, *J* 7.1), 3.84 (s, 2 H, NCH₂), 2.86 (s, 6 H, NMe₂), 1.28 (t, 6 H, CH₂CH₃, *J* 7.1), 1.25 (t, 6 H, CH₂CH₃, *J* 7.1). Positive-ion FAB mass spectrum: *m/z* 399 (M⁺).

X-ray Structure Determination of 3, 5, and 8. Crystals suitable for a diffraction study were grown from toluene/hexane (complexes **3** and **5**) or dichloromethane/hexane (complex **8**). Details of data collection and refinement are given in Table 4.

Acknowledgment. Financial support of this work by the DGES (project PB97-1036), Spain, is acknowledged. V.R. thanks CajaMurcia, Spain, for a research grant.

Supporting Information Available: Tables of crystal data and refinements details, atomic coordinates and equivalent isotropic displacement parameters, complete bond distances and angles, and ORTEP views for compounds **3**, **5**, and **8**. This material is available free of charge via the Internet at <http://pubs.acs.org>.

OM0008600